SUPPLEMENTAL INFORMATION

Structural and Molecular Basis for Coordination in a Viral DNA Packaging Motor

Huzhang Mao, Mitul Saha, Emilio Reyes-Aldrete, Michael B. Sherman, Michael Woodson, Rockney Atz, Shelley Grimes, Paul J. Jardine, Marc C. Morais

Supplemental Figure S1

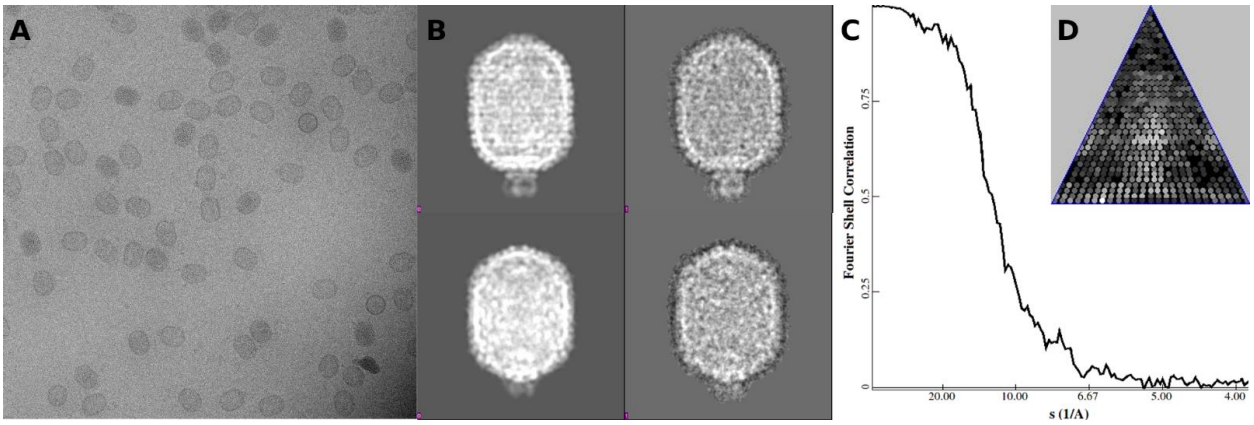

Figure S1, related to Figure 3: **Cryo-EM data of phi29 particles stalled during packaging via the addition of γ-S-ATP**. A) Original micrograph of particles stalled during packaging. B) Comparisons of class averages of particles with corresponding projections of the final model. Approximately side and tilted views of packaging particles are shown in the top and bottom panels, respectively. A thresh-hold based mask with a soft Gaussian fall-off was applied to each class average. C) FSC curve comparing independent half-data sets; the correlation drops below 0.5 at ~ 12 Å resolution. D) Distribution of particle orientations in the C5 asymmetric unit; the pixel brightness reflects the number of particles with a particular orientation on a logarithmic scale. The sampling of points in the asymmetric unit was down-sampled, and thus is coarser than the angular intervals between projections during refinement to facilitate viewing.

Supplemental Figure S2

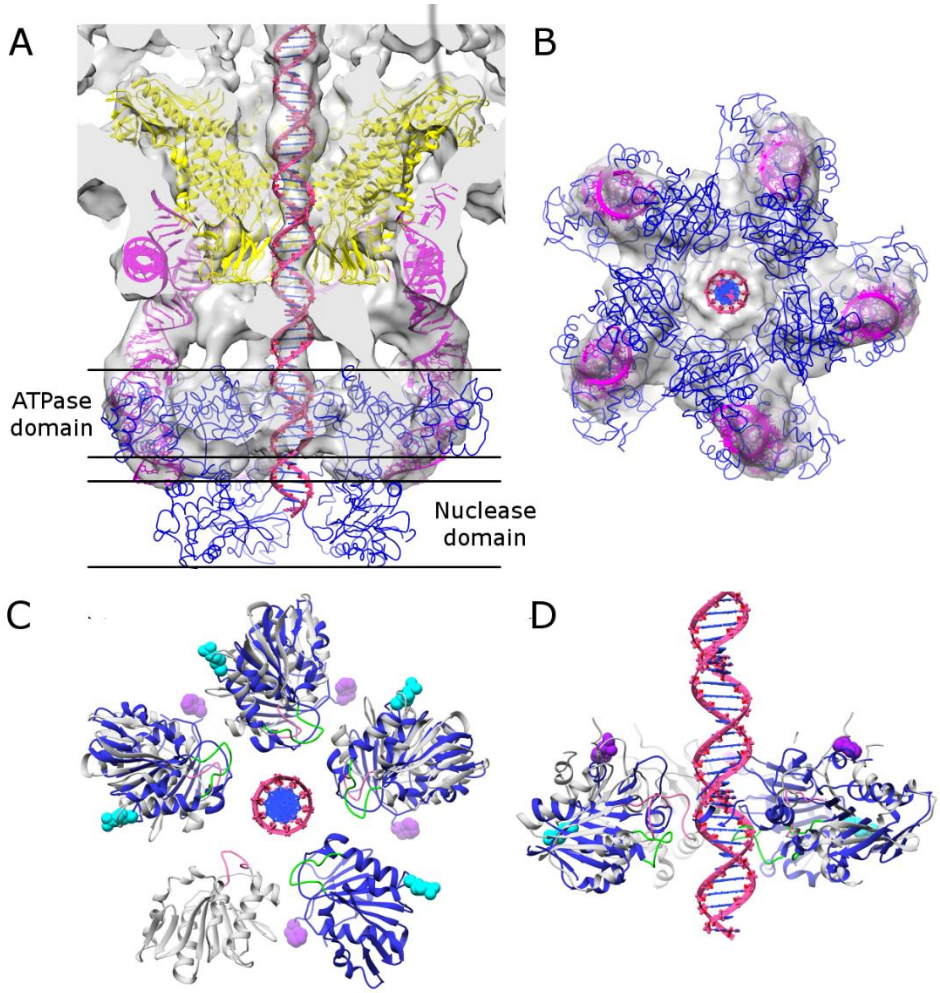

Figure S2, related to table 3: Comparison of the bacteriophage phi29 and other ASCE motors. A) Cut-away side view of the cryoEM reconstruction of the bacteriophage phi29 dsDNA packaging motor with the atomic coordinates of the T4 ATPase gp17 (blue wire; PDB 3EZK) fitted into density corresponding to phi29 ATPase gp16. The orientation of the T4 motor relative to the capsid is as in Sun et al. (Sun et al., 2008). Although the ATPase domain of T4 gp17 is at the same level as the ATPase domain of gp16, there would be extensive clashes with the pRNA (magenta); the C-terminal nuclease domain is out of density below the domain. The phi29 connector and DNA are shown in yellow and red, respectively. B) End-on view of the T4 ATPase fitted into cryoEM density of the phi29 packaging motor; the direction of view is from below the phage looking towards the interior of the capsid. C) End-on view of a superposition of Ftsk-based (blue) and P4-based (grey) pentameric rings of gp26. One subunit has been left out of each ring to facilitate viewing. The arginine finger and C-terminus of the construct are shown as cyan and purple spheres in the Ftsk-based ring; the DNA translocating loops in the Ftsk- and P4-based rings are colored green and pink, respectively. DNA is shown in red. D) Side view of superposition of Ftsk-based and P4-based pentameric rings of gp16, with the front half of the rings removed to facilitate viewing.

Supplemental Figure S3

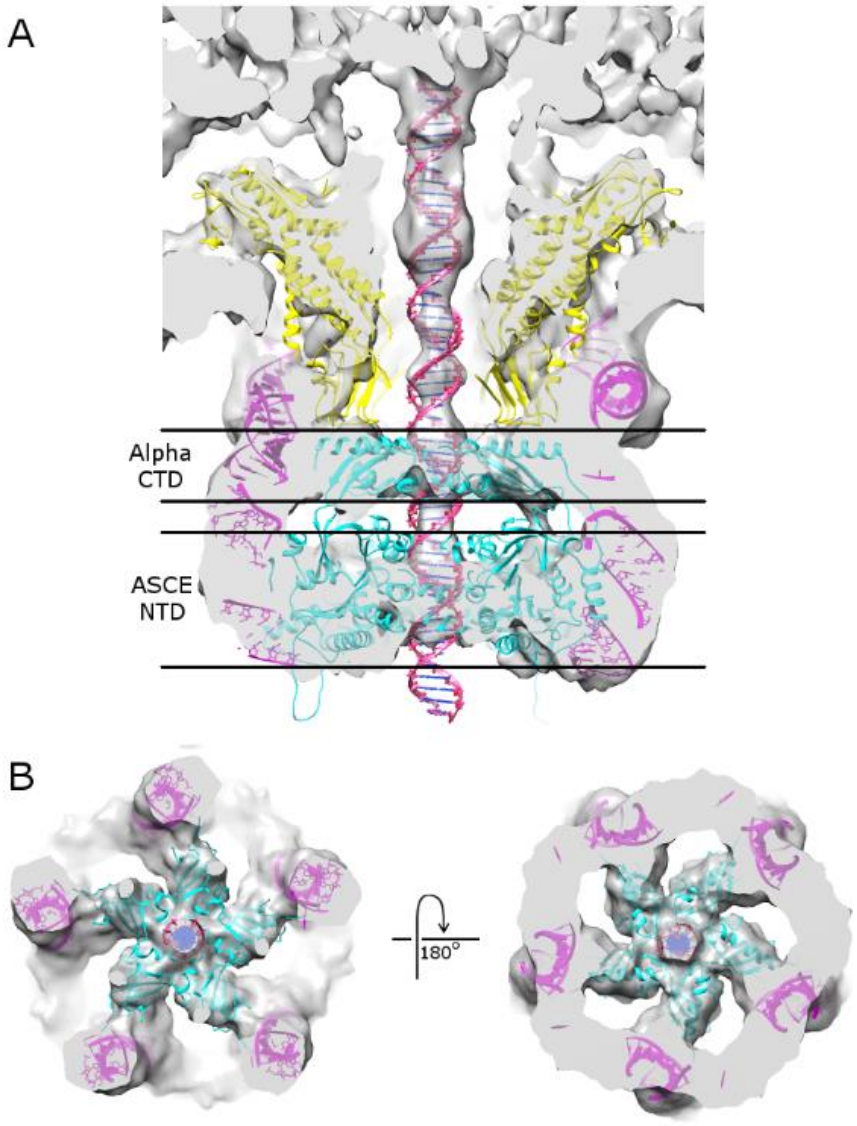

Figure S3, related to Figure 2. **The relative arrangement of N- and C-terminal domains in gp16 and Ftsk is similar.** A) Cut-away side view of the cryoEM reconstruction of the bacteriophage phi29 dsDNA packaging motor with the atomic coordinates of five copies of the full-length FtsK (cyan; PDB 2IUU) positioned based on super-position of the N-terminal ASCE domain of FtsK on the ASCE domain of gp16. The approximate levels of the N- and C-terminal domains are indicated. Note that this arrangement of full-length Ftsk monomers positions the C-terminal α-domain of Ftsk in density assigned to the C-terminal domain of gp16. The connector and DNA are colored yellow and red, respectively. B) Cut-away end-on views of the FtsK CTDs in density corresponding to the gp16 CTDs (see also contact 2, Figure 3b and d) viewed from outside the phage looking in (left) and inside the phage looking out (right).

Supplemental Figure S4

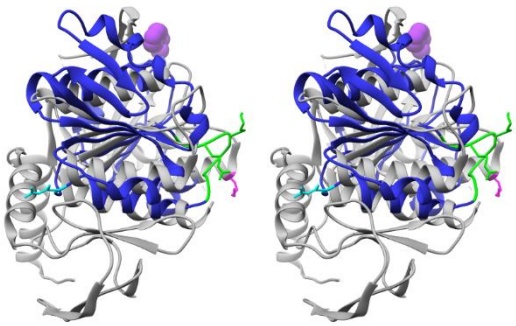

Figure S4, related to Table 3. **The DNA translocating loop in gp16 is structurally homologous to the translocating lever in the P4 packaging motor.** Cross-eyed stereo diagram of gp16 (blue) superimposed on P4 (grey). The putative DNA translocating loop in gp16 (green) is analogous to the RNA translocating lever in P4 (indicated by an essential lysine shown in pink). Residues R122 and/or K124 in gp16 are shown as green stick figures; these residues were shown to be required for DNA translocation, but do not affect ATP hydrolysis. The arginine finger R146 and the C-terminal F196 are shown as cyan stick and purple spheres, respectively.

Supplemental Figure S5

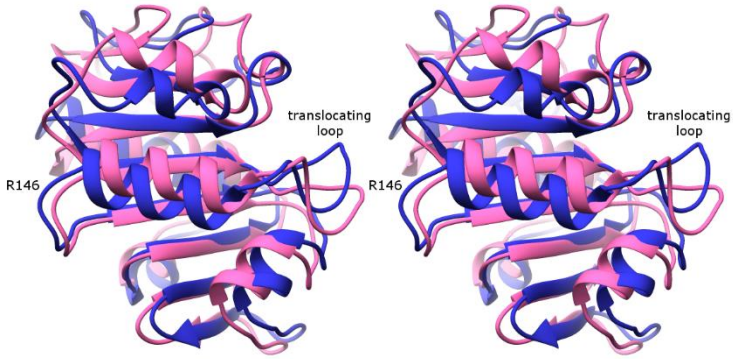

Figure S5, related to Figure 2. Normal mode analysis of gp16 indicates that motions of the arginine finger and DNA translocating loop are coupled. Cross-eyed stereo diagram of two NMA-generated conformers of gp16 colored blue and pink, respectively. The locations of the DNA translocating loop and arginine finger R146 are indicated. The amplitude of the motion is arbitrary; NMA analyses such as this only show the direction of molecular motions. Normal modes were calculated using the web-based NMA server AD-ENM (http://enm.lobos.nih.gov/) ((Zheng and Doniach, 2003)

SUPPLEMENTAL REFERENCES

Sun, S., Kondabagil, K., Draper, B., Alam, T.I., Bowman, V.D., Zhang, Z., Hegde, S., Fokine, A., Rossmann, M.G., and Rao, V.B. (2008). The structure of the phage T4 DNA packaging motor suggests a mechanism dependent on electrostatic forces. Cell *135*, 1251-1262.

Zheng, W., and Doniach, S. (2003). A comparative study of motor-protein motions by using a simple elastic-network model. Proc Natl Acad Sci U S A *100*, 13253-13258.